

# Synchronization transitions in ensembles of noisy oscillators with bi-harmonic coupling

Vladimir Vlasov,<sup>1</sup> Maxim Komarov,<sup>1,2</sup> and Arkady Pikovsky<sup>1,2</sup>

<sup>1</sup>*Institute for Physics and Astronomy,*

*University of Potsdam, 14476 Potsdam, Germany*

<sup>2</sup>*Department of Control Theory, Nizhni Novgorod State University,*

*Gagarin Av. 23, 606950, Nizhni Novgorod, Russia*

(Dated: May 2, 2018)

## Abstract

We describe synchronization transitions in an ensemble of globally coupled phase oscillators with a bi-harmonic coupling function, and two sources of disorder - diversity of intrinsic oscillatory frequencies and external independent noise. Based on the self-consistent formulation, we derive analytic solutions for different synchronous states. We report on various non-trivial transitions from incoherence to synchrony where possible scenarios include: simple supercritical transition (similar to classical Kuramoto model), subcritical transition with large area of bistability of incoherent and synchronous solutions, and also appearance of symmetric two-cluster solution which can coexist with regular synchronous state. Remarkably, we show that the interplay between relatively small white noise and finite-size fluctuations can lead to metastable asynchronous solution.

## I. INTRODUCTION

In the theory of synchronization, Kuramoto model of globally coupled phase oscillators [1–3] is one of the most popular setups for describing synchronization phenomena. The case of a harmonic sin-coupling function is well studied in literature [2, 4, 5]. However, when reducing complex nonlinear oscillatory dynamics to relatively simple phase models, one often has to deal with multiharmonic coupling functions [2]. In this paper we concentrate on the particular case of the Kuramoto model of globally coupled phase oscillators with a bi-harmonic interaction function. Such type of interaction between oscillators arises in several realistic physical setups including: (i) classical Huygens’ setup with pendulum clocks suspended on a common beam with both vertical and horizontal displacements [6, 7]; (ii) recently experimentally observed  $\varphi$ -Josephson junctions, where the dynamics of a single junction in the array is governed by a double-well energy potential [8]; (iii) globally coupled electrochemical oscillators [9, 10], where the second harmonics has been obtained from the experimental data.

In our work we take into account two main sources of disorder that hinder synchronization, namely diversity of oscillators’ frequencies, and white additive noise acting on the phases. Recent theoretical studies indicate that in the noise-free case the Kuramoto model with bi-harmonic coupling function is characterized by a variety of multi-branch entrainment modes [11–13]. The latter manifests itself as a multiplicity (multistability) of different synchronous states, with distinct redistributions of oscillators between two stable branches of microscopic dynamics [7, 14]. In this work we show that the action of white noise removes the multiplicity, however, the overall picture of transitions from incoherence to synchrony is non-trivial and can be quite complex in comparison to the standard Kuramoto model.

The paper is organized as follows. First, we formulate the problem and perform a special, suitable for the analysis, parametrization of the system. Then, we present a self-consistent approach allowing us to find order parameters in dependence on the coupling constants and disorder in an analytic form. Wherever possible, we perform the stability analysis. And at last, we discuss the limiting case of small noise intensity and its relation to the noiseless situation. In conclusion, we summarize and collect all the findings together.

## II. BASIC MODEL

In this paper we study an ensemble of phase oscillators (phase variables  $\phi_k$ ), subject to a mean-field bi-harmonic coupling and noise [in this formulation we use “primed” variables, which will be in short transformed to dimensionless ones]:

$$\frac{d\phi_k}{dt'} = \omega_k \Delta' + \frac{\varepsilon}{N} \sum_{j=1}^N \sin(\phi_j - \phi_k) + \frac{\gamma}{N} \sum_{j=1}^N \sin(2\phi_j - 2\phi_k) + \sqrt{D'} \xi_k(t'). \quad (1)$$

Here  $\omega_k$  are normalized natural frequencies of oscillators that are assumed to have a symmetrical distribution  $g(\omega)$  with unit width and zero mean value (the latter condition is not a restriction, as it can be always achieved by transforming to a properly rotating reference frame). Parameter  $\Delta'$  measures the spread of the distribution of natural frequencies. Gaussian white noise is defined according to  $\langle \xi_k(t'_1) \xi_j(t'_2) \rangle = 2\delta(t'_1 - t'_2) \delta_{kj}$ . Parameters  $\varepsilon$  and  $\gamma$  define the strength of the coupling on the first and the second harmonics, respectively.

Eq. (1) can be rewritten as

$$\frac{d\phi_k}{dt'} = \omega_k \Delta' + \varepsilon R_1 \sin(\Theta_1 - \phi_k) + \gamma R_2 \sin(\Theta_2 - 2\phi_k) + \sqrt{D'} \xi_k(t'), \quad (2)$$

where  $R_m e^{i\Theta_m} = N^{-1} \sum_j e^{im\phi_j}$ ,  $m = 1, 2$ , are the two relevant order parameters.

Eq. (2) has 4 parameters, all of them of dimension  $1/t'$ :  $\Delta', \varepsilon, \gamma, D'$ . By rescaling time, one parameter can be set to one. We choose to set the overall coupling  $\varepsilon + \gamma$  to unity. Thus, we introduce  $t = (\varepsilon + \gamma)t'$  and get

$$\dot{\phi}_k = \omega_k \Delta + q R_1 \sin(\Theta_1 - \phi_k) + (1 - q) R_2 \sin(\Theta_2 - 2\phi_k) + \sqrt{D} \xi(t), \quad (3)$$

where  $\Delta = \Delta'/(\varepsilon + \gamma)$ ,  $q = \varepsilon/(\varepsilon + \gamma)$  and  $D = D'/(\varepsilon + \gamma)$ . Parameter  $q$  describes relation between coupling coefficients  $\varepsilon$  and  $\gamma$ , such that the case  $q = 0$  corresponds to a pure second harmonic coupling with  $\varepsilon = 0$ , while  $q = 1$  corresponds to a pure Kuramoto-type first harmonic coupling with  $\gamma = 0$ . In this new normalization, increasing or decreasing of coupling strength is equivalent to decreasing or increasing of the disorder parameters  $\Delta$  (spread of frequencies) and  $D$  (noise), while keeping a constant relation  $\Delta/D$  between them. This suggests to introduce new parameters  $T, s$  in such a way that  $\Delta = (1 - s)T$ ,  $D = sT$ . Therefore, parameter  $T$  measures the overall disorder (noise plus spread of frequencies), normalized by the overall coupling strength  $\varepsilon + \gamma$ . Parameter  $s$  measures the relation between parameters  $\Delta$  (width of frequency distribution) and  $D$  (noise): for  $s = 0$  the system is

purely deterministic, while for  $s = 1$  it describes an ensemble of identical noisy oscillators. Summarizing, Eq. (3) with new parameters  $q, T, s$  becomes

$$\dot{\phi}_k = \omega_k(1-s)T + qR_1 \sin(\Theta_1 - \phi_k) + (1-q)R_2 \sin(\Theta_2 - 2\phi_k) + \sqrt{sT}\xi_k(t). \quad (4)$$

We consider the thermodynamic limit  $N \rightarrow \infty$ , then the order parameters are just ensemble averages  $R_m e^{i\Theta_m} = \langle e^{im\phi} \rangle$  and in the thermodynamical limit can be represented through the conditional probability density function of the phases  $\rho(\varphi|\omega)$ , as

$$R_m e^{i\Theta_m} = \langle e^{im\varphi} \rangle = \int \int g(\omega) \rho(\varphi|\omega) e^{im\varphi} d\varphi d\omega \quad (5)$$

In thermodynamic formulation we use the variable  $\varphi$  to describe the phase and skip all indices, therefore, according to (4) the equation for the phase variable  $\varphi$  at given  $\omega$  reads

$$\frac{d\varphi}{dt} = \omega(1-s)T + qR_1 \sin(\Theta_1 - \varphi) + (1-q)R_2 \sin(\Theta_2 - 2\varphi) + \sqrt{sT}\xi(t). \quad (6)$$

The Fokker-Planck equation for  $\rho(\varphi, t|\omega)$  follows from Eq. (6):

$$\frac{\partial \rho}{\partial t} + \frac{\partial}{\partial \varphi} \left[ \left( \omega(1-s)T + qR_1 \sin(\Theta_1 - \varphi) + (1-q)R_2 \sin(\Theta_2 - 2\varphi) \right) \rho \right] = sT \frac{\partial^2 \rho}{\partial \varphi^2}. \quad (7)$$

The limiting noise-free case when  $s = 0$  has been described in details in [7, 14]. In this paper we will present a general analysis for systems with noise and a finite distribution of frequencies. We will treat the limit  $s \ll 1$ , which appears to be singular, separately. The other limiting case  $s = 1$  is the case of the identical natural frequencies, in terms of the analysis presented below it is not special. However, for  $s = 1$  an additional stability analysis can be performed, thus this case will be also considered in details separately.

### III. STATIONARY SOLUTIONS: SELF-CONSISTENT APPROACH

A disordered state with a uniform distribution of phases  $\rho = (2\pi)^{-1}$  and vanishing order parameters  $R_1 = R_2 = 0$  is always a solution of the system (5,7). Additionally, we expect nontrivial synchronized states of two types: (i) all order parameters are non-zero, and (ii) a symmetric 2-cluster distribution where all odd order parameters vanish  $R_{2m+1} = 0$  and  $R_{2m} \neq 0$ ,  $m \in \mathbb{N}_0$ .

### A. Solution in a parametric form

Due to the symmetry of the coupling function and of the distribution of natural frequencies  $g(\omega)$ , the nontrivial solutions are stationary states (what means that the frequency of the mean fields is exactly the average oscillator frequency) with  $\Theta_1 = \Theta_2 = 0$ . Thus, the stationary conditional probability density function  $\rho(\varphi | \omega)$  satisfies the stationary Fokker-Planck equation

$$\frac{\partial}{\partial \varphi} \left[ \left( \omega(1-s) - \frac{qR_1}{T} \sin(\varphi) - \frac{(1-q)R_2}{T} \sin(2\varphi) \right) \rho \right] = s \frac{\partial^2 \rho}{\partial \varphi^2}, \quad (8)$$

where because of symmetry

$$R_m = \int \int g(\omega) \rho(\varphi | \omega) \cos(m\varphi) d\varphi d\omega \quad (9)$$

To find the solutions of this self-consistent system explicitly, it is convenient to introduce two new auxiliary variables  $R$  and  $\alpha$  (together with definitions  $u$ ,  $v$ , and  $x$ ) according to

$$\begin{aligned} R &= \sqrt{\left( \frac{qR_1}{T} \right)^2 + \left( \frac{(1-q)R_2}{T} \right)^2}, \\ u &= \cos \alpha = \frac{qR_1}{TR}, \\ v &= \sin \alpha = \frac{(1-q)R_2}{TR}, \\ x &= \frac{\omega}{R} \end{aligned} \quad (10)$$

Then the stationary Fokker-Planck equation (8) for the stationary distribution density  $\rho(\varphi | x)$  (which depends on  $R$ ,  $\alpha$ ,  $s$  as parameters) reads

$$\frac{\partial}{\partial \varphi} \left[ R \left( x(1-s) - u \sin(\varphi) - v \sin(2\varphi) \right) \rho \right] = s \frac{\partial^2 \rho}{\partial \varphi^2}. \quad (11)$$

An explicit solution of (11) can be written as double integrals, but practically it is more convenient to solve it in the Fourier modes representation

$$\rho(\varphi | x) = \frac{1}{2\pi} \sum_n C_n(\alpha, R, s, x) e^{in\varphi}, \quad C_n(\alpha, R, s, x) = \int_0^{2\pi} \rho e^{-in\varphi} d\varphi, \quad C_0 = 1. \quad (12)$$

Substituting (12) in Eq. (11) we obtain

$$\begin{aligned} 0 &= \int_0^{2\pi} \left[ -\frac{\partial}{\partial \varphi} \left[ R \left( x(1-s) - u \sin(\varphi) - v \sin(2\varphi) \right) \rho \right] + s \frac{\partial^2 \rho}{\partial \varphi^2} \right] e^{-ik\varphi} d\varphi = \\ &= R \left[ \left( -ix(1-s)k - k^2 s/R \right) C_k + ik u \frac{C_{k-1} - C_{k+1}}{2i} + ik v \frac{C_{k-2} - C_{k+2}}{2i} \right]. \end{aligned} \quad (13)$$

Thus, from (13) we obtain a system of linear algebraic equations for the mode amplitudes:

$$2\left(ix(1-s) + ks/R\right)C_k + u(C_{k+1} - C_{k-1}) + v(C_{k+2} - C_{k-2}) = 0, \quad (14)$$

which can be solved by standard methods after a proper truncation to a finite number of Fourier modes (which controls accuracy of the solution) is performed. After finding  $C_{1,2}(\alpha, R, s, x)$ , we have to calculate integrals

$$F_{1,2}(\alpha, R, s) = \int g(Rx) \operatorname{Re} [C_{1,2}(\alpha, R, s, x)] dx. \quad (15)$$

This allows us to represent the order parameters as

$$R_{1,2}(\alpha, R, s) = R \int g(Rx) \operatorname{Re} [C_{1,2}(\alpha, R, s, x)] dx = RF_{1,2}(\alpha, R, s). \quad (16)$$

Substituting this in Eq. (10), we obtain our parameters  $T, q$  as functions of the auxiliary variables

$$\begin{aligned} T &= \frac{1}{\frac{\cos \alpha}{F_1} + \frac{\sin \alpha}{F_2}}, \\ q &= \frac{\frac{\cos \alpha}{F_1}}{\frac{\cos \alpha}{F_1} + \frac{\sin \alpha}{F_2}} = \frac{1}{1 + \frac{F_1}{F_2} \tan \alpha}. \end{aligned} \quad (17)$$

Summarizing, we have obtained the explicit solution of the self-consistent problem: for each fixed  $s$ , by varying  $\alpha \in [0, \pi/2]$  and  $R \in [0, \infty)$ , we obtain the solution in a parametric form:  $R_{1,2} = R_{1,2}(\alpha, R)$  according to (16),  $T = T(\alpha, R)$  and  $q = q(\alpha, R)$  according to (17).

The case of purely two-cluster state with  $R_1 = 0$  corresponds to  $\alpha = \pi/2$ , it is singular in (16,17). Here the solution is represented as

$$R_2 = RF_2, \quad T = (1 - q)F_2. \quad (18)$$

Thus, by the method presented above, it is possible to find stationary solutions of the Eq. (7) for any given  $q, T$  and  $s$ . In the general case of  $s < 1$ , Eq. (7) is integro-differential equation and the analysis of the stability of all solutions is quite difficult, except for the simplest incoherent solution  $\rho = (2\pi)^{-1}$ . However, in the limiting case of identical natural frequencies  $s = 1$ , density  $\rho$  is  $\omega$ -independent, and integration in (9) over frequencies gives always 1. This means that Fourier modes (12) are in fact the order parameters:  $R_m(q, T, 1) = \operatorname{Re} [C_m(q, T, 1, 0)]$ . The same is valid also for the full time-dependent problem: it can be written as a system of nonlinear ordinary differential equations for time-dependent Fourier modes of the density, which can be analyzed for stability after a proper truncation. Thus, we start with this particular case.

## B. Limiting case of identical oscillators

Here we describe the case of identical natural frequencies, what means that  $\Delta = (1-s)T = 0$  or  $s = 1$ . As discussed above, in this case also a stability analysis is possible, which we outline below. First, let us represent Eq. (7) in terms of Fourier modes  $C_m$  which are related to the complex order parameters  $C_m^* = R_m e^{i\Theta_m}$  (the procedure is the same as in obtaining (13)):

$$\frac{dC_k}{dt} = -k^2 T C_k + kq \frac{C_1 C_{k-1} - C_1^* C_{k+1}}{2} + k(1-q) \frac{C_2 C_{k-2} - C_2^* C_{k+2}}{2}. \quad (19)$$

We are interested in stability of a stationary solution, obtained according to (16,17) or (18).

For the linear stability analysis, a small perturbation around stationary solution  $\tilde{C}_k$  should be added, thus we set  $C_k = \tilde{C}_k + c_k$  in Eq. (19), and in the first order in  $c_k$  obtain

$$\begin{aligned} \frac{dc_k}{dt} = & -k^2 T c_k + \frac{kq}{2} \left( c_1 \tilde{C}_{k-1} - c_1^* \tilde{C}_{k+1} \right) + \\ & + \frac{k(1-q)}{2} \left( c_2 \tilde{C}_{k-2} - c_2^* \tilde{C}_{k+2} + \tilde{C}_2 c_{k-2} - \tilde{C}_2^* c_{k+2} \right), \end{aligned} \quad (20)$$

Equation (20) is an infinite system, but because the amplitudes of modes with large  $k$  tend to zero, it is possible to truncate it at some large  $N$ , and to write a finite system of Eqs. (20), with  $k$  varying from 1 to  $N$ , where  $N$  is large enough. By finding a maximum eigenvalue of the corresponding matrix for values  $q$  and  $T$  of interest, it is possible to find stability properties of the solution  $\tilde{C}_k$  and build the boundary  $q = q(T)$  where the solution  $\tilde{C}_k$  changes its stability. This can be done both for general solutions (16,17) and for the two-cluster states (18).

We present the diagram of synchronous states in the parameter plane  $(q, T)$ , for the case of identical oscillators  $s = 1$  in the Fig. 1. Here also the stability lines of the disordered state  $\rho = (2\pi)^{-1}$  are shown with dashed lines (see Appendix A for details of calculation). Three major states can be observed: a disordered one, one with all non-zero order parameters, and a two-cluster one where all odd order parameters vanish. For small and large values of parameter  $q$ , i.e. where one of the coupling modes dominates (the first harmonics coupling for  $q$  close to one or the second harmonics coupling for  $q$  close to zero) the transitions are supercritical. We illustrate them in Fig. 2 (panels (a),(d)), showing dependencies of the order parameters on  $T$ . In the middle part of the phase diagram (between the points marked  $p_1, p_2$  in Fig. 1), for  $q$  close to 0.3, the transitions are subcritical, so that a bistability occurs.

These regimes are illustrated in Fig. 2 (panels (b),(c)). Transition from the disordered to the two-cluster state is always supercritical (see dashed red line in panels (c,d) of Fig. 2).

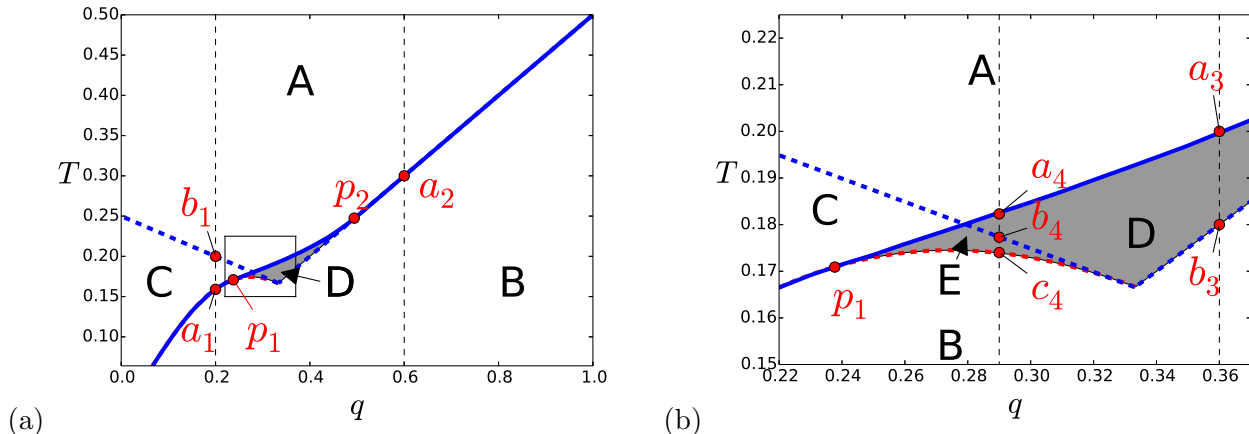


FIG. 1. (a) Different regimes in the parameter plane  $(q, T)$  are shown for  $s = 1$ . Area A: asynchronous solution. Area B: coherent regime with  $R_{1,2} \neq 0$ . Area C: two-cluster coherent regime with only order parameter  $R_2 \neq 0$ ,  $R_1 = 0$ . Area D: region of bistability of incoherent and synchronous solutions. Area E: bistability of the two-cluster state and a state with  $R_{1,2} \neq 0$ . Dashed blue lines are stability lines of the disordered state, obtained from (A11) and (A12). Between the points  $p_1$  and  $p_2$  the transition is hysteretic; dashed red line is the stability line of Area C, obtained from (20), it coincides with the line where on the branch existing for small  $T$  the first order parameter tends to zero. (b) Enlarged central region of panel (a). Vertical dashed lines are cuts of the diagram illustrated in Fig. 2.

### C. General phase diagram

The phase diagrams on plane of basic parameters  $(q, T)$  for other values of  $s$  are qualitatively the same as Fig. 1. We show two cases  $s = 0.1$  and  $s = 0.5$  in Fig. 3. All these diagrams are qualitatively similar, and we expect also that stability properties of different solutions are like in Fig. 2.



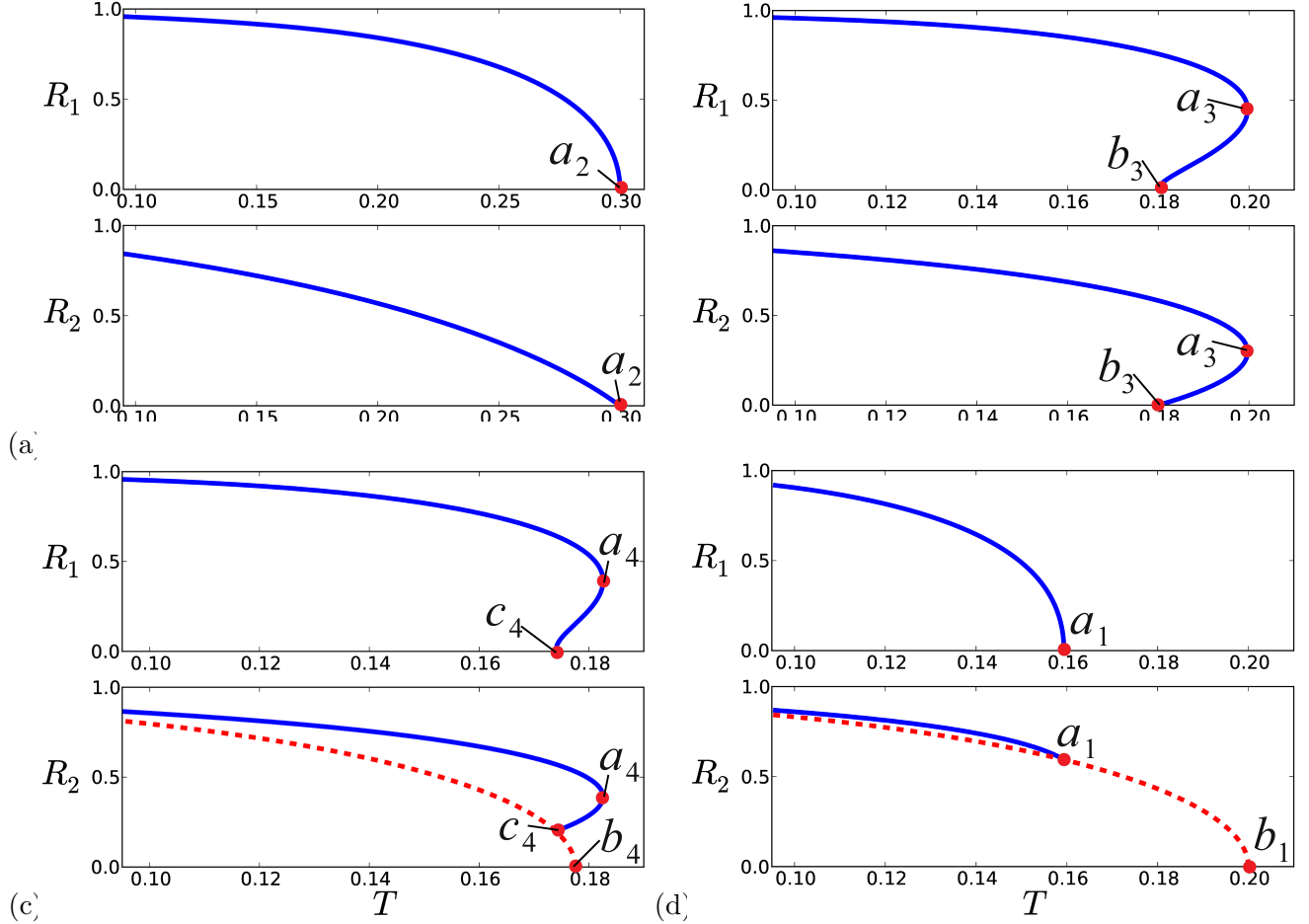


FIG. 2. Dependencies of order parameters  $R_{12}$  on the disorder parameter  $T$ , for  $s = 1$  and different values of  $q$ : (a)  $q = 0.9$ , (b)  $q = 0.36$ , (c)  $q = 0.28$ , (d)  $q = 0.2$ . Solid blue line: branch of general solution  $R_1 \neq 0$ ; dashed red line: branch of the two-cluster state with  $R_1 = 0$ ,  $R_2 \neq 0$ .

#### IV. LIMITING CASE OF SMALL NOISE

In this section we describe the limit of small noise  $s \rightarrow 0$ , that corresponds to the noise-free case of bi-harmonic Kuramoto model studied in [7, 11, 12, 14–16]. This is the mostly challenging part, both numerically and theoretically. Numerically, there is a problem in finding a stationary probability density from (11), because this density becomes close to a delta-function, i.e. first a large number of Fourier modes is needed, and second the methods of solving an algebraic system for these modes converge very slowly. Theoretically, it is known that for a noise-free case, there is a multiplicity of solutions coexisting with a neutrally stable disordered state [14], this degeneracy is lifted by adding an arbitrary small noise. The reason for this singular limit is that the Fokker-Planck equation behaves singularly in the

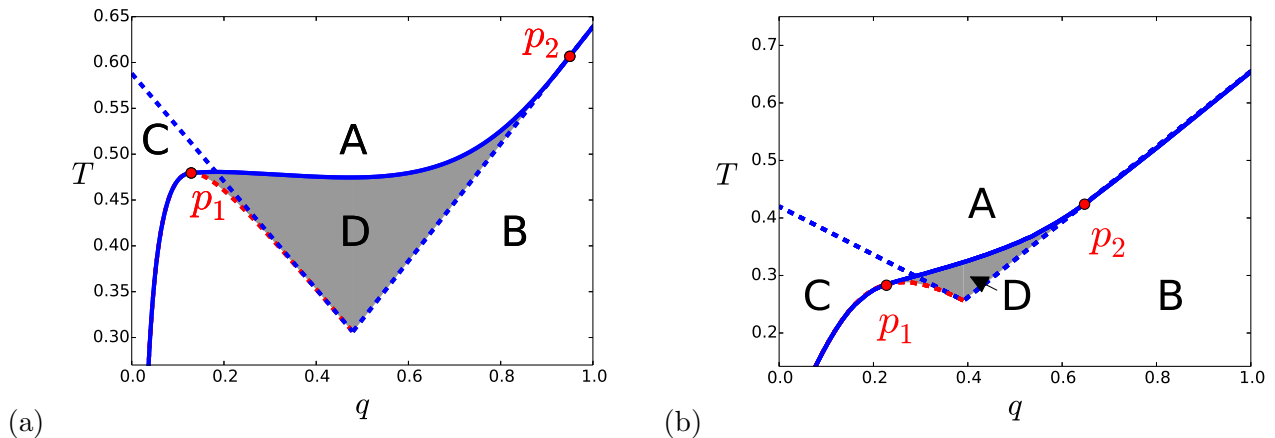


FIG. 3. The same as Fig. 1, but for  $s = 0.1$  (a) and  $s = 0.5$  (b). Region E is not denoted because it is very thin on these plots.

limit of small noise: while for any noise the stationary distribution is unique, in the noise-free case the order of equation is reduced and there are multiple solutions of the resulting Liouville equation.

In order to shed light on the limit  $s \rightarrow 0$ , we fixed  $q = 0.5$ , and calculated dependencies  $R_{1,2}(T)$  for  $s = 0$  using the approach described in [7] for the noise-free case, and the approach above for different values of parameter  $s$ . The results presented in Fig. 4 show how the noise-free curve (dashed red curve in fig. 4(a)) is approached as  $s \rightarrow 0$  (solid curves in Fig. 4). One can see that there is a jump in the values of  $T$  at which the curves touch the line  $R_{1,2} = 0$ . For the case of noisy oscillators, these points are those where the disordered state loses its stability. For the noise-free case, it is another point, not related to a stability exchange. This jump is responsible for a formation of a “boundary layer”, depicted in more details in Fig. 4(b), where the noisy curves rapidly escape the vicinity of the curve  $s = 0$  as  $R_{1,2}$  go to zero. It appears that the solution of the limiting case  $s = 0$  always differs significantly from the noisy solutions  $s \neq 0$  at  $R \rightarrow 0$ , regardless of the noise strength represented by the parameter  $s$ .

In the other words, the limit  $s \rightarrow 0$  for the noisy case does not coincide with the noise-free solution  $s = 0$  near the bifurcation point  $R = 0$ . This effect was also discussed in the papers [7, 14]. In the limiting noise-free case  $s = 0$ , the stationary solutions for distribution function  $\rho(\varphi, \omega)$  are always singular: they contain combination of delta-functions for any small  $R_{1,2}$  (see [7] for detail). In contradistinction, the presence of the noise always regularizes solutions

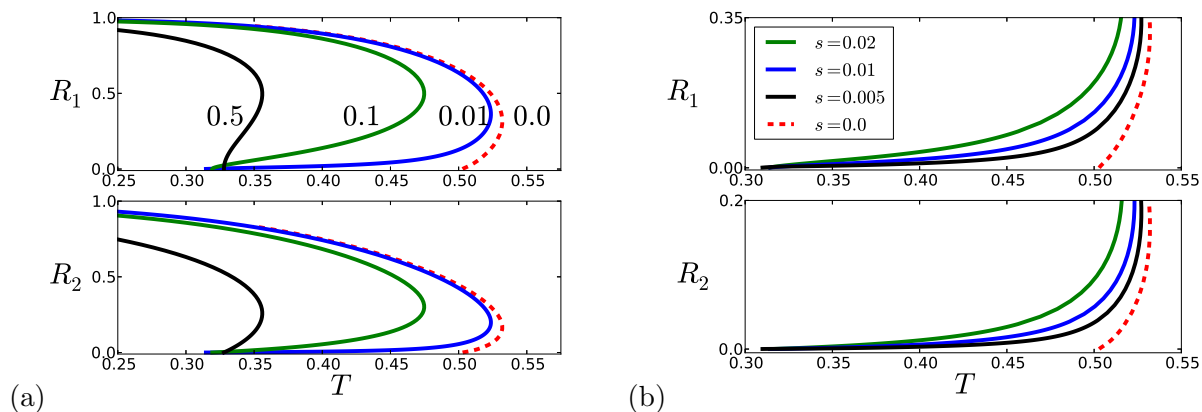


FIG. 4. (a) The dependencies of order parameters  $R_{1,2}$  on the overall disorder  $T$  for  $q = 0.5$  and different values of  $s$ . The numbers on the upper panel depict values of  $s$ : from the left curve to the right one  $s$  changes from 0.5 to zero. The dashed curve corresponds to the special case of  $s = 0.0$ . (b) The same as in (a) but now curves are plotted near the points of transition from incoherent to synchronous solutions ( $R \rightarrow 0$ ).

causing smooth and non-singular stationary distribution functions  $\rho(\varphi, \omega)$ . It is important to notice, that the effective noise appears as a combination  $s/R$  in the algebraic equations for stationary modes (14). Therefore, for any  $s \neq 0$  we always have the limit of effectively “large noise” at the bifurcation point  $R \rightarrow 0$ . The latter causes qualitative difference near the transition point  $R \rightarrow 0$  between noisy ( $s \neq 0$ ) and noise-free ( $s = 0$ ) cases even for infinitely small noise strength. With decrease of  $s$ , the “boundary layer” shrinks (the smaller is parameter  $s$ , the smaller values  $R$  we need for effective noise to be large) as one can see from Fig. 4.

Remarkably, the incoherent state which is linearly stable in the thermodynamic limit, can become metastable for finite-size ensembles in the region of bistability of asynchronous and synchronous solutions. As one can see from the figure 4(a,b), the lower branch of synchronous solutions (the unstable one) is relatively close to the incoherent state  $R_{1,2} = 0$  at the point  $T = 0.47$ . Therefore, due to the random finite-size fluctuations, there is always a probability for the system to escape the small basin of attraction of the disordered state, and to make a transition to synchronous state which has a much larger basin. The figure 5 shows statistics of the life times  $\tau$  of the incoherent solution (linearly stable in thermodynamical limit) for relatively small noise strength  $s = 0.01$  and  $T = 0.47$ . For each value of  $N$  we performed

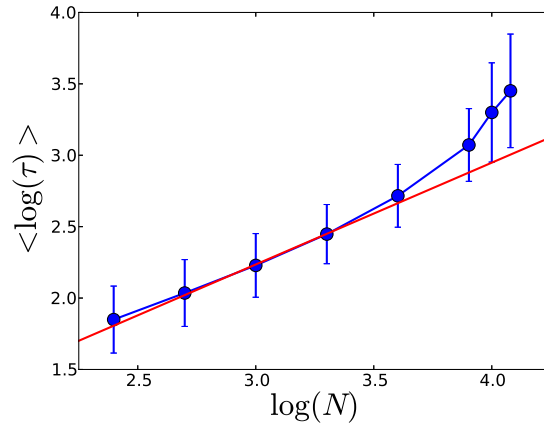


FIG. 5. Statistics of the transition time from the incoherent state (linearly stable in thermodynamic limit) to synchronous mode for the finite size ensemble. Parameters:  $q = 0.5$ ,  $T = 0.47$ ,  $s = 0.01$ .

many runs, from which the mean value  $\langle \log \tau \rangle$  and the standard deviation of  $\log \tau$  has been calculated (so that the errorbars in Fig. 5 are not due to insufficient averaging but represent the variability of the life times).

The averaged time of transition increases as number of oscillators in the system grows. Remarkably, one can see on Fig. 5 a crossover from a regime of a power-law dependence of the life time on the system size (for  $N \lesssim 4000$  a relation  $\tau \sim N^{0.71}$  holds) to a more rapid decrease of the life time for  $N \gtrsim 8000$ . We have to compare this with the noise-free case, where according to [7] the life time scales as  $\sim N^{0.72}$ . One can see that for small system size, i.e. for large finite-size fluctuations, the noise-free situation is reproduced. We explain this as following: small noise makes the asynchronous state only weakly stable, compared to neutral stability of the noise-free case, and for large finite-size fluctuations these weak stability is not seen. For smaller fluctuations, the system starts to see the “potential barrier” to overcome to go into the stable state with large order parameter. Now the life time is the activation time which can be expected to follow an exponential Kramers’ law for very small fluctuations (regime, not accessible for moderate values of  $N$  that we are able to study numerically). This explains the crossover observed in Fig. 5.

## V. CONCLUSION

The paper is devoted to the investigation of the Kuramoto model of globally coupled oscillators with bi-harmonic coupling function. In particular, here we concentrated on the effects caused by the action of the independent additive white noise forces on the oscillators. In the first part of the paper we have formulated the self-consistent theory that allows one to find stationary solutions for the system in the thermodynamic limit (when number of oscillators goes to infinity) in the presence of noise and an arbitrary distribution of frequencies. As a result of the developed theory, we calculated general bifurcation diagram and described all possible stationary regimes of the model, for different values of noise strength, spread of frequencies distribution, and coupling constants.

In the noise-free case, as has been shown in [7, 14], there exists a multiplicity (multistability) of the coherent states due to the presence of the second harmonics in the coupling. In this work we have shown that the action of white noise withdraws the multiplicity, however the noise causes several additional complications to the bifurcation diagram.

First of all, due to the noise, the model contains large area of parameters with so-called “nematic phase”, which represents synchronous two-cluster state with zero first order parameter ( $R_1 = 0$ ,  $R_2 \neq 0$ ). Depending on the parameter values, the transitions to synchrony can be complicated, where possible scenarios include:

- a simple supercritical (second-order) transition to synchrony, where both order parameters scale as a square root of supercriticality. This case is similar to the standard Kuramoto model with pure sinusoidal coupling and occurs when the second harmonics coupling is relatively small;
- a subcritical (first-order) transition to synchrony, with a large area of bistability of coherent and asynchronous solutions. This type of transition becomes dominating as noise strength goes to zero and the second harmonics in the coupling function remains relatively strong;
- first a two-cluster state appears via a supercritical (second-order) transition. This state is characterized by zero first order parameter and square-root scaling of the second order parameter. As disorder decreases, a general synchronous state appears via a subcritical (first-order) transition. This happens in the case of relatively weak

first harmonic in the coupling function;

- first a two-cluster state appears via a supercritical (second-order) transition. As disorder decreases, a general synchronous state appears via a supercritical (second-order) transition, at which the amplitude of the first order parameter grows continuously. This happens in the case of very small first harmonics term in the coupling function.

We also report on the finite-size-induced transitions to synchrony for finite ensembles. As it was mentioned before, in the thermodynamic limit the transition to synchrony can be hysteretic with large area of bistability of synchronous and asynchronous solutions when the second harmonic is relatively large. In the latter case, noise causes a transition from incoherent state (linearly stable in the thermodynamic limit) to synchronous solution for finite-size ensembles.

Finally, we would like to mention an analogy of our model of coupled oscillators with bi-harmonic coupling to a popular in statistical mechanics XY-model of globally coupled spins with ferromagnetic and nematic coupling [17, 18]. In the latter context the desynchronized state is a disordered one, while one-cluster and two-cluster states are ferromagnetic and nematic ones. Two main differences are: (i) in the context of statistical mechanics, stability of solutions is established via the minimization of free energy in the canonical description or maximization of entropy in the microcanonical one, while in the dynamical formulation above stability properties are defined locally; (ii) diversity of oscillators' frequencies is a non-equilibrium feature not appearing in the equilibrium formulation of the XY model (cf. [19] for a comparison of the Kuramoto model with corresponding models from statistical physics).

## ACKNOWLEDGMENTS

V.V. thanks the IRTG 1740/TRP 2011/50151-0, funded by the DFG/FAPESP. M. K. thanks Alexander von Humboldt foundation and the Russian Science Foundation (Project No. 14-12-00811) for support. A. P. acknowledges the Galileo Galilei Institute for Theoretical Physics (Florence, Italy) for the hospitality and the INFN for partial support during the completion of part of this work, and supported by the grant (agreement 02.49.21.0003 of August 27, 2013 between the Russian Ministry of Education and Science and Lobachevsky State University of Nizhni Novgorod)

## Appendix A: Stability analysis of the incoherent solution

The detail stability analysis of the incoherent solution of the system of phase equations with multi-harmonic coupling function has been performed in [20, 21]. Here we will present the analysis in the particular case of bi-harmonic coupling function in the new parameter plane  $(q, T, s)$ .

Consider the following Fokker-Planck equation (7) for conditional probability density function  $\rho(\varphi, t | \omega)$

$$\frac{\partial \rho}{\partial t} + \frac{\partial}{\partial \varphi} \left[ \left( \omega(1-s)T + q \operatorname{Im}(Z_1 e^{-i\varphi}) + (1-q) \operatorname{Im}(Z_2 e^{-2i\varphi}) \right) \rho \right] = sT \frac{\partial^2 \rho}{\partial \varphi^2}, \quad (\text{A1})$$

where

$$Z_m(t) = \int \int g(\omega) \rho(\varphi, t | \omega) e^{im\varphi} d\varphi d\omega. \quad (\text{A2})$$

Then in the Fourier modes representation

$$\rho(\varphi, t | \omega) = \frac{1}{2\pi} \sum_n C_n(t, \omega) e^{in\varphi} \quad C_n(t, \omega) = \int_0^{2\pi} \rho e^{-in\varphi} d\varphi, \quad C_0(t, \omega) = 1 \quad (\text{A3})$$

we obtain

$$\begin{aligned} \frac{dC_k}{dt} &= \int_0^{2\pi} \left[ -\frac{\partial}{\partial \varphi} \left[ \left( \omega(1-s)T + q \operatorname{Im}(Z_1 e^{-i\varphi}) + (1-q) \operatorname{Im}(Z_2 e^{-2i\varphi}) \right) \rho \right] + sT \frac{\partial^2 \rho}{\partial \varphi^2} \right] e^{-ik\varphi} d\varphi = \\ &= \left( -ik\omega(1-s)T - k^2 sT \right) C_k + ikq \frac{Z_1^* C_{k-1} - Z_1 C_{k+1}}{2i} + ik(1-q) \frac{Z_2^* C_{k-2} - Z_2 C_{k+2}}{2i}. \end{aligned} \quad (\text{A4})$$

Thus we obtain the following system for  $C_k$

$$\frac{dC_k}{dt} = k \left[ -\left( i\omega(1-s)T + ksT \right) C_k + q \frac{Z_1^* C_{k-1} - Z_1 C_{k+1}}{2} + (1-q) \frac{Z_2^* C_{k-2} - Z_2 C_{k+2}}{2} \right], \quad (\text{A5})$$

where

$$Z_{1,2}(t) = \int g(\omega) C_{1,2}^*(t, \omega) d\omega. \quad (\text{A6})$$

Small perturbation to incoherent solution  $\rho(\varphi, t | \omega) = (2\pi)^{-1}$  means that  $C_k \ll 1$  for  $k \neq 0$  and thus  $Z_m \ll 1$ , so in order to linearize the system (A5) we can neglect all the terms such as  $C_m C_n$  and  $Z_m C_n$  and higher. Then for  $k > 0$

$$\begin{aligned} \frac{dC_1}{dt} &= -T \left( i\omega(1-s) + s \right) C_1 + q \frac{Z_1^*}{2}, \\ \frac{dC_2}{dt} &= -2T \left( i\omega(1-s) + 2s \right) C_2 + (1-q) Z_2^*, \\ \frac{dC_k}{dt} &= -kT \left( i\omega(1-s) + ks \right) C_k, \quad \text{for } k = 3, 4, \dots \end{aligned} \quad (\text{A7})$$

and complex conjugate equations for  $k < 0$  because  $C_{-k} = C_k^*$ . Introduction to (A7) of the expressions (A6) for  $Z_{1,2}$  gives integro-differential equations for  $C_{1,2}$

$$\begin{aligned}\frac{dC_1}{dt} &= -T\left(i\omega(1-s) + s\right)C_1 + q\frac{1}{2}\int g(\omega)C_1 d\omega, \\ \frac{dC_2}{dt} &= -2T\left(i\omega(1-s) + 2s\right)C_2 + (1-q)\int g(\omega)C_2 d\omega, \\ \frac{dC_k}{dt} &= -kT\left(i\omega(1-s) + ks\right)C_k, \quad \text{for } k = 3, 4, \dots\end{aligned}\tag{A8}$$

From (A8) follows that the equations for the harmonics split and because  $T \geq 0$  and  $0 \leq s \leq 1$  all the high harmonics with  $k \geq 3$  and their complex conjugates are stable, whereas instability appears in first and second harmonics independently, depending on  $q, T$ .

Since the equations for modes (A8) are decoupled in order to find boundary conditions when the first and second harmonics become unstable one should put in (A8)  $dC_1/dt = 0$  and  $dC_2/dt = 0$  and self-consistently obtain two conditions on the parameters  $q, T$ . Then, by using expression (A6) we obtain

$$\begin{aligned}T\left(i\omega(1-s) + s\right)C_1 &= q\frac{1}{2}Z_1^*, \\ 2T\left(i\omega(1-s) + 2s\right)C_2 &= (1-q)Z_2^*.\end{aligned}\tag{A9}$$

Introducing (A9) to (A6)

$$\begin{aligned}Z_1^* &= \frac{q}{2T}\int \frac{g(\omega)Z_1^*}{i\omega(1-s) + s} d\omega, \\ Z_2^* &= \frac{1-q}{2T}\int \frac{g(\omega)Z_2^*}{i\omega(1-s) + 2s} d\omega,\end{aligned}\tag{A10}$$

we obtain two lines on the  $(q, T)$  parameter plane for any given  $s$ :

$$T = q\frac{1}{2}\int \frac{g(\omega)s}{\omega^2(1-s)^2 + s^2} d\omega,\tag{A11}$$

and

$$T = (1-q)\int \frac{g(\omega)s}{\omega^2(1-s)^2 + 4s^2} d\omega.\tag{A12}$$

Where the line (A11) on the  $(q, T)$  plane corresponds to the linear stability boundary for  $R_1 = 0$  and another line (A12) corresponds to the linear stability boundary for  $R_2 = 0$ .

---

[1] Y. Kuramoto, in *International Symposium on Mathematical Problems in Theoretical Physics*, edited by H. Araki (Springer Lecture Notes Phys., v. 39, New York, 1975) p. 420.



- [2] Y. Kuramoto, *Chemical Oscillations, Waves and Turbulence* (Springer, Berlin, 1984).
- [3] J. A. Acebrón, L. L. Bonilla, C. J. P. Vicente, F. Ritort, and R. Spigler, *Rev. Mod. Phys.* **77**, 137 (2005).
- [4] E. Ott and T. M. Antonsen, *CHAOS* **18**, 037113 (2008).
- [5] E. Ott and T. M. Antonsen, *CHAOS* **19**, 023117 (2009).
- [6] K. Czołczyński, P. Perlikowski, A. Stefański, and T. Kapitaniak, *Communications in Nonlinear Science and Numerical Simulation* **18**, 386 (2013).
- [7] M. Komarov and A. Pikovsky, *Physica D* **289**, 18 (2014).
- [8] E. Goldobin, D. Koelle, R. Kleiner, and R. G. Mints, *Phys. Rev. Lett.* **107**, 227001 (2011).
- [9] I. Z. Kiss, Y. Zhai, and J. L. Hudson, *Phys. Rev. Lett.* **94**, 248301 (2005).
- [10] I. Z. Kiss, Y. Zhai, and J. L. Hudson, *Prog. Theor. Phys. Suppl.* **161**, 99 (2006).
- [11] H. Daido, *J. Phys. A: Math. Gen.* **28**, L151 (1995).
- [12] H. Daido, *Phys. Rev. Lett.* **77**, 1406 (1996).
- [13] A. T. Winfree, *The Geometry of Biological Time* (Springer, Berlin, 1980).
- [14] M. Komarov and A. Pikovsky, *Phys. Rev. Lett.* **111**, 204101 (2013).
- [15] H. Chiba and I. Nishikawa, *Chaos* **21**, 043103 (2011).
- [16] K. Li, S. Ma, H. Li, and J. Yang, *Phys. Rev. E* **89**, 032917 (2014).
- [17] T. N. Teles, F. P. d. C. Benetti, R. Pakter, and Y. Levin, *Phys. Rev. Lett.* **109**, 230601 (2012).
- [18] A. Pikovsky, S. Gupta, T. Teles, F. Benetti, R. Pakter, Y. Levin, and S. Ruffo, *arXiv:1410.2219* (2014).
- [19] M. Komarov, S. Gupta, and A. Pikovsky, *EPL* **106**, 40003 (2014).
- [20] J. D. Crawford, *Phys. Rev. Lett.* **74**, 4341 (1995).
- [21] J. D. Crawford and K. T. R. Davies, *Physica D* **125**, 1 (1999).